引用格式：鄢继华, 蒲秀刚, 侯中帅, 等. 黄骅坳陷石炭系—二叠系煤系页岩沉积特征及富气潜力[J]. 油气藏评价与开发, 2025, 15(6): 1007-1016.
YAN Jihua, PU Xiugang, HOU Zhongshuai, et al. Sedimentary characteristics and gas enrichment potential of Carboniferous-Permian coal-measure shale in Huanghua Depression[J]. Petroleum Reservoir Evaluation and Development, 2025, 15(6): 1007-1016.
DOI: 10.13809/j.cnki.cn32-1825/te.2025.06.006

黄骅坳陷石炭系—二叠系煤系页岩沉积特征及富气潜力

鄢继华[1], 蒲秀刚[2], 侯中帅[3], 陈世悦[1]
（1.中国石油大学（华东）地球科学与技术学院，山东 青岛 266580；2.中国石油大港油田公司，天津 300280；3.河北地质大学能源研究所，河北 石家庄 050031）

摘要：为了给渤海湾盆地煤系油气勘探突破提供理论支撑，以黄骅坳陷太原组—山西组页岩为研究对象，利用岩心、薄片、测井、录井和有机地球化学资料，厘定了页岩发育的沉积环境类型，明确了目的层段页岩的沉积演化特征，分析了不同沉积环境页岩的有机地球化学特征，确定页岩气勘探的有利层段。研究结果表明：黄骅坳陷太原组—山西组页岩形成于障壁海岸和三角洲环境，其中太原组下段页岩发育潟湖亚相，上段发育潮坪亚相；山西组下段页岩发育水下分流河道间微相，上段发育分流间湾微相。黄骅坳陷太原组—山西组页岩自下而上总体经历了由障壁海岸相到三角洲相的转变，指示着晚古生代海侵作用由高峰转向衰退的演化过程。页岩有机质丰度以障壁海岸相最高，其次为三角洲相，不同沉积相页岩的有机质类型相近，干酪根均以Ⅲ型为主，包含部分$Ⅱ_2$型，有机质总体处于低成熟—成熟的演化阶段。太原组上段的潮坪页岩为页岩气勘探的有利层段，沧县隆起、东光潜山和北大港潜山等地区是页岩气勘探的有利区。

关键词：黄骅坳陷；石炭系—二叠系；煤系页岩；沉积环境；沉积有机质
中图分类号：TE122　　**文献标识码：**A

Sedimentary characteristics and gas enrichment potential of Carboniferous-Permian coal-measure shale in Huanghua Depression

YAN Jihua[1], PU Xiugang[2], HOU Zhongshuai[3], CHEN Shiyue[1]

(1. School of Geosciences, China University of Petroleum (East China), Qingdao, Shandong 266580, China; 2. PetroChina Dagang Oil Company , Tianjin 300280, China; 3. Energy Research Institute, Hebei GEO University, Shijiazhuang, Hebei 050031, China)

Abstract: Shale is at the forefront of oil and gas geological research and a hotspot for exploration; however, research has mainly focused on marine and lacustrine shale systems, while studies on shale within transitional coal-measure strata are relatively limited. The Carboniferous-Permian coal-measure strata in the Bohai Bay Basin are well-developed, characterized by widely distributed, regionally stable, and thick shale layers. These strata represent excellent source rocks and reservoirs, indicating significant potential for oil and gas exploration and development. This study investigated the coal-measure shale of the Carboniferous-Permian Taiyuan and Shanxi Formations in the Huanghua Depression of the Bohai Bay Basin. Using data from core analysis, thin sections, well logging, organic carbon content, Rock-Eval pyrolysis, and vitrinite reflectance (R_0), this study examined the depositional environment types of coal-measure shale, the vertical evolution of the depositional environments, and the organic geochemical properties of the shale from different depositional environments. This research aims to provide a theoretical basis for oil and gas exploration in the Carboniferous-Permian coal-measure strata of the Bohai Bay Basin. The Carboniferous-Permian coal-measure strata in the Huanghua Depression were divided into the Taiyuan Formation and the Shanxi Formation. The Taiyuan Formation was mainly characterized by barrier coastal facies, while the Shanxi Formation was dominated by deltaic facies. The shale of the Taiyuan Formation was primarily deposited in lagoon and tidal flat environments of the barrier coastal system, whereas the shale of the Shanxi Formation was mainly deposited in subaqueous distributary channels and interdistributary bay environments of the deltaic system. The lithological and logging characteristics of shale from different sedimentary facies were identified. Lagoon shale was gray-black, with well-developed horizontal laminations. Under the microscope, felsic material was visible, with fine particle sizes generally

收稿日期：2024-10-03。
第一作者简介：鄢继华（1977—），男，博士，副教授，主要从事沉积学及层序地层学等方面研究。地址：山东省青岛市黄岛区长江西路66号中国石油大学（华东），邮政编码：266580。E-mail：upcyanjihua@sina.com
基金项目：国家科技重大专项“渤海湾盆地深层油气地质与增储方向”（2016ZX05006-007）。

at the silt grade. Brownish-red siderite concretions were common, often exhibiting irregular ellipsoidal shapes with their long axes typically aligned parallel to the bedding planes. Lagoon shale exhibited distinct logging responses, characterized by high natural gamma and high resistivity on conventional logs, and bright yellow to bright red backgrounds with faint lamination structures on image logs. Tidal flat shale was mainly deposited in tidal flat environments. It was predominantly gray to black or dark gray. In core samples, well-developed felsic bands with a thickness of approximately 1 mm were visible. These felsic bands were laterally discontinuous and tapered off within the core samples. The particles within the bands were fine-grained, mainly silt-sized. Compared to lagoon shale, the tidal flat shale exhibited significantly lower resistivity. In imaging logs, the color appeared noticeably darker. The low response was attributed to the development of felsic bands within the tidal flat shale. The interbedding of thin sand and mud layers resulted in individual shale layers that were thinner than the vertical resolution of resistivity logging tools, leading to the measured apparent resistivity values being lower than the true formation resistivity. Consequently, the resistivity of tidal flat shale in the study area was significantly lower than that of the lagoon shale. Shale in subaqueous distributary channels was dark gray to gray-black and contained abundant siderite concretions occurring in banded and irregularly massive forms. These concretions mainly consisted of microcrystalline siderite grains, with minor felsic detrital particles, and were commonly associated with carbonaceous debris. Carbon and oxygen isotope analyses indicated that the formation of siderite in the delta front was influenced by organic matter and the water chemistry of the depositional environment. After deposition in the delta front, terrestrial carbonaceous debris decomposed, releasing CO_3^{2-}, which combined with Fe^{2+} in the pore water to form siderite. The water coverage in the delta front also provided favorable conditions for siderite development. The abundant siderite in the shale reduced the formation conductivity and radioactive element content, resulting in low resistivity, uranium, and thorium readings on logs. Conversely, the high photoelectric absorption cross-section (P_e) of siderite increased the P_e value of the formation. Shale in interdistributary bays exhibited diverse colors, including dark gray, gray, and variegated colors, indicating strong water-level fluctuations during deposition and the presence of both subaqueous and emergent environments. Siderite was less developed in the interdistributary bay shale. Consequently, its resistivity and radioactive element content were significantly higher, and its P_e value was significantly lower than those of the subaqueous distributary channel shale. The depositional evolution of the Taiyuan and Shanxi Formations recorded a transition from the peak of the Late Paleozoic marine transgression to subsequent regression. Consequently, the depositional environments of shale transitioned from barrier coastal to deltaic facies, with shale sequentially developing in lagoon, tidal flat, delta front, and delta plain subfacies from bottom to top. The measured total organic carbon content of the shale varied among depositional environments: lagoon shale (0.11%～19.30%, avg. 3.81%), tidal flat shale (0.70%～17.99%, avg. 4.18%), subaqueous distributary channel shale (0.29%～5.91%, avg. 2.45%), and interdistributary bay shale (0.03%～7.36%, avg. 2.21%). A comparison showed that the tidal flat shale had the highest average total organic carbon abundance, followed by lagoon shale, subaqueous distributary channel shale, and interdistributary bay shale. Overall, the organic matter abundance of shale from barrier coastal facies was higher than that from deltaic facies. The organic matter types of shales from different depositional environments were similar, primarily Type III kerogen with some Type II_2, indicating a mixed input of terrestrial higher plants and aquatic lower organisms, with terrestrial higher plants being the dominant source. The measured R_0 values ranged from 0.60% to 1.12%, indicating that the organic matter was generally in a low-maturity to mature stage. The total organic carbon abundance of tidal flat shale (avg. 4.18%) was slightly higher than that of lagoon shale and significantly higher than that of deltaic shales, making it favorable for shale gas generation. The higher content of felsic particles in tidal flat shale enhanced the development of macropores and micropores, which were beneficial for shale gas storage. Meanwhile, the felsic particles increased the brittle mineral content, thereby enhancing the stimulation potential of the shale. Gas logging data also indicated gas-rich intervals within the shale. Overall, the Taiyuan Formation exhibited stronger gas logging responses than the Shanxi Formation, and tidal flat shale outperformed lagoon shale. These characteristics indicated that the tidal flat shale in the upper Taiyuan Formation was the most promising gas-rich interval. During the Early Permian deposition of the upper Taiyuan Formation, the marine transgression in North China mainly originated from the southeast. Tidal flat deposits were extensively developed across most of the Huanghua Depression, while barrier islands and lagoon deposits were confined to the eastern Chenghai area. Tidal flats were primarily distributed in the western part of the Huanghua Depression, with a northeast-southwest trend. Within this trend, the Cangxian uplift, Dongguang, Wumaying, Kongdian, Beidagang, Qibei, and Qinan buried hills were identified as favorable areas for shale gas exploration.

Keywords: Huanghua Depression; Carboniferous-Permian; coal-measure shale; sedimentary environment; sedimentary organic matter

页岩是现今油气地质研究的前沿领域[1-2],也是油气勘探的热点[3-5],诸多学者针对其岩相类型、沉积环境与模式、有机地球化学等特征进行了研究[6-10],但研究工作主要集中在海相页岩和湖相页岩层系[11-12],针对过渡相煤系地层中页岩的研究相对较少。渤海湾盆地石炭系—二叠系中过渡相煤系地层十分发育,该层系中页岩厚度大,分布范围广且在区域上稳定发育。近年来,渤海湾盆地石炭系—二叠系油气勘探过程中发现了多个原生油气藏[13-14],同时邻近的鄂尔多斯盆地也在煤系页岩气勘探领域取得突破[15],指示着其可以作为良好的烃源岩和储

集层，具有巨大的油气勘探开发潜力。渤海湾盆地石炭系—二叠系中煤系地层发育的沉积环境多样[16]，对于不同沉积背景下页岩的沉积特征、垂向演化以及有机地球化学特征的研究较为匮乏。以渤海湾盆地黄骅坳陷石炭系—二叠系中的煤系页岩为研究对象，利用岩心、薄片、测录井、有机碳、热解和镜质体反射率等资料，对煤系页岩发育的沉积环境类型及特征、煤系页岩沉积环境的垂向演化以及有机地球化学特征进行研究，以期为渤海湾盆地石炭系—二叠系中煤系油气资源勘探提供一定的基础支撑。

1　区域地质概况

黄骅坳陷为渤海湾盆地中部的一个中新生代断坳复合盆地，其西北以沧东断层为界，与沧县隆起相接，东南与埕宁隆起呈超覆与断层的过渡关系，东侧为沙垒田凸起。黄骅坳陷在平面上具有向西南收敛，向北东海域撒开的不对称狭长状的形态特征（图1a），总面积约为18 000 km^2，其中，陆上面积约为11 000 km^2[17-18]。

黄骅坳陷中的石炭系—二叠系在经历了中新生代的构造活动改造后保存仍较为完好，位于石炭系—二叠系下部的煤系地层在坳陷内分布广泛，其自下而上可分为本溪组、太原组和山西组（图1b）。太原组底部以半沟灰岩的顶面为与本溪组的分界面，在晋祠砂岩发育的地区，则以晋祠砂岩的底面为与本溪组的分界面。太原组顶部以6号煤的顶面为与山西组的分界面，太原组中部发育的8+9号煤的底面为太原组下段和上段分界面，太原组下段岩性主要为灰黑色页岩夹砂岩、灰岩和煤层，测井上总体具有高自然伽马和高电阻率的特征，太原组上段岩性主要为砂岩与页岩互层夹煤层和灰岩，煤层的发育程度较太原组下段高，测井上总体具有低自然伽马和低电阻率的特征。山西组顶部以骆驼脖子砂岩的底面为与上覆下石盒子组的分界面，山西组中部发育的3号煤的底面为山西组下段和上段分界面，在3号煤不发育的地区

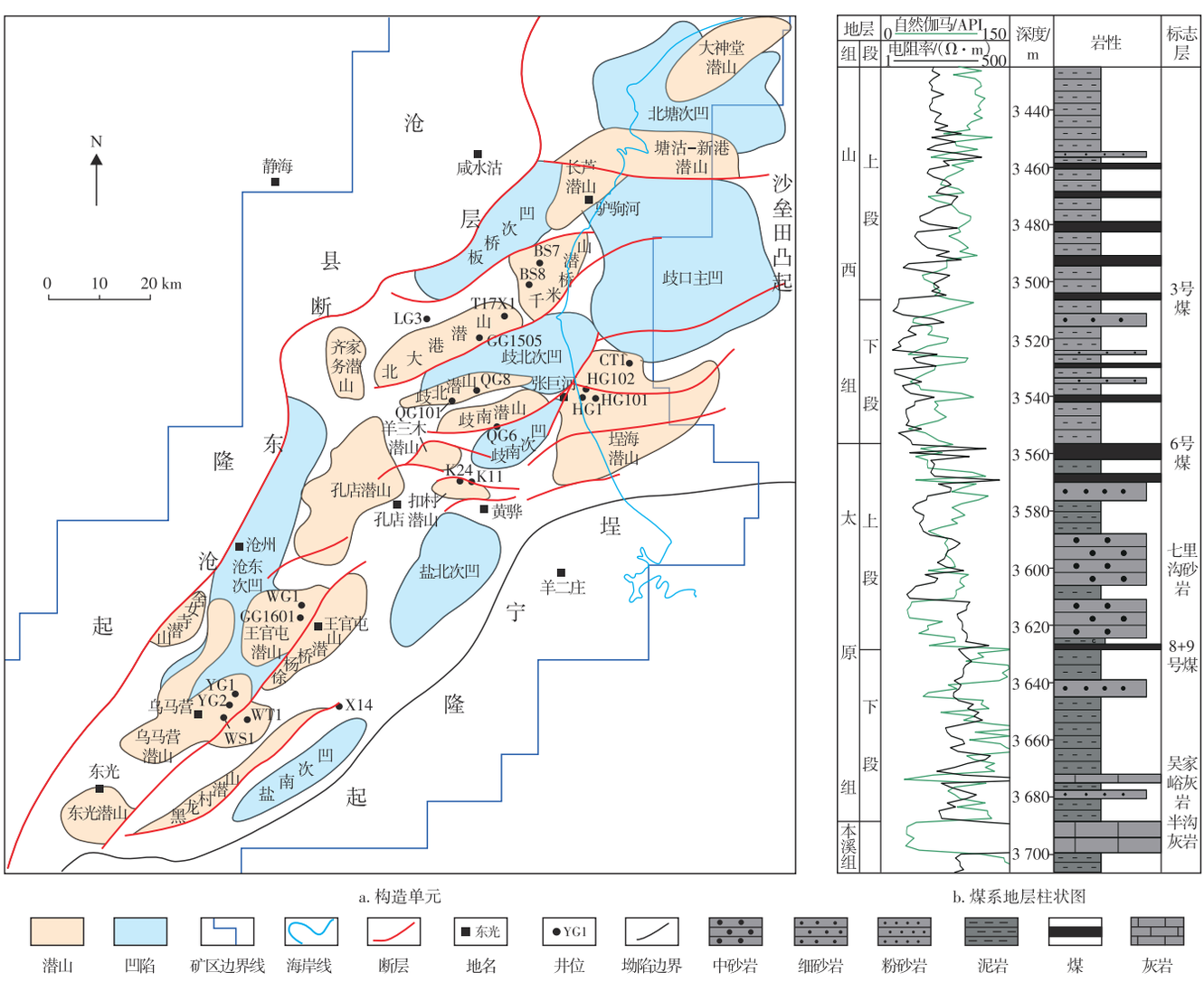

图1　黄骅坳陷构造单元与煤系地层柱状图

Fig. 1　Structural units and coal-measure stratigraphic column of Huanghua Depression

则以船窝砂岩的底面为分界面，山西组下段岩性主要为深灰色页岩夹砂岩和煤层，测井上总体具有低电阻率的特征，山西组上段岩性主要为深灰色、灰色页岩夹砂岩和煤层，煤层的发育程度明显较下段高，测井上总体具有中高自然伽马和中高电阻率的特征。

2　页岩沉积环境

黄骅坳陷太原组—山西组中页岩主要发育在障壁海岸相和三角洲相中，其中障壁海岸相中发育页岩的亚相包括潟湖和潮坪，三角洲相中发育页岩的亚相包括三角洲前缘和三角洲平原。不同亚相中页岩的颜色、沉积构造、自生矿物类型和测井响应具有一定的差异性。

2.1　潟湖

潟湖为受障壁岛或古地形影响而与广海分隔的局限海湾环境。潟湖亚相中主要发育灰黑色页岩（图2a），岩石中水平层理较为发育，镜下可见页岩中含有部分长英质物质，其粒度较细，总体在粉砂级别。潟湖页岩中常见褐红色菱铁矿结核，其常具有不规则椭球状的外形，长轴方向通常与层面一致。镜下观察发现菱铁矿结核主要由微晶和粉晶菱铁矿晶粒组成，夹有少量背景沉积物中的黏土矿物和长英质矿物等陆源碎屑物质。潟湖页岩的测井响应特征明显，在常规测井中表现出高自然伽马和高电阻率的特点，在成像测井上整体具有亮色背景，呈明显的亮黄色和亮红色，并表现出不明显的纹层结构（图3a）。

2.2　潮坪

潮坪为在平缓的古地形背景下发育的受潮汐作用控制的沉积类型，研究区潮坪中页岩主要发育在泥坪微相中。泥坪微相主要发育灰黑色和深灰色页岩，岩心中可见页岩中长英质条带十分发育，其厚度一般在1 mm左右（图2b）。长英质条带在横向上分布不稳定，岩心中可见其发生横向尖灭，条带中颗粒的粒度较细，主要为粉砂级。长英质条带在垂向上与泥质层频繁互层出现，形成透镜状层理，指示着泥坪发育期水体深度变化较为频繁。

相对于潟湖页岩，泥坪页岩具有明显的低电阻率的特点，成像测井上表现出明显的暗色背景和黑色条带模式（图3a），这种响应特征与泥坪页岩中长英质条带的发育有关，砂泥岩薄互层的发育会使得单层页岩的厚度常低于电阻率测井仪器的纵向分辨率，使得测量的视电阻率值常大大低于地层的真实电阻率[19]，最终造成研究区泥坪页岩的测井电阻率明显低于潟湖页岩。

2.3　三角洲前缘

研究区三角洲发育在陆表海背景下[14]，前缘亚相主要由水下分流河道和水下分流河道间微相组成，其中页岩主要发育在水下分流河道间微相中。

水下分流河道间主要发育深灰色和灰黑色页岩，页岩中菱铁矿结核十分发育，主要以条带状和不规则团块状的形式产出（图2c）。镜下观察发现结核主要由微晶菱铁矿晶粒组成，其中夹有少量长英质碎屑颗粒，同时普遍与炭屑相伴生。碳氧同位素分析表明三角洲前缘菱铁矿的形成受沉积有机质和环境水体的影响[20]，陆源炭屑在三角洲前缘沉积后分解释放出CO_3^{2-}，其与水体中的Fe^{2+}结合后形成菱铁矿，同时三角洲前缘的覆水环境也为菱铁矿的发育提供了有利条件。

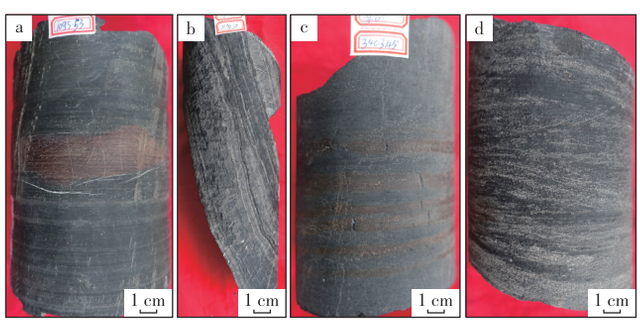

注：a为灰黑色页岩含菱铁矿结核，潟湖，太原组下段，C19井，1 095.33 m；b为透镜状层理，潮坪，太原组上段，DT1井，2 490.50 m；c为深灰色页岩中发育菱铁矿条带，三角洲前缘，山西组下段，DG1井，3 403.45 m；d为深灰色页岩中砂质含量高，三角洲平原，山西组上段，X14井，2 787.43 m。

图2　不同环境页岩岩石学与沉积学特征

Fig. 2　Petrological and sedimentological characteristics of shales from different sedimentary environments

菱铁矿的大量发育使得水下分流河道间页岩的岩石物理性质具有明显的特征，具体表现在：①易导电的菱铁矿降低了地层的电阻率，造成其在测井上常表现出低电阻率的特征；②在菱铁矿密集发育的井段，地层中放射性元素的含量受到稀释，在自然伽马能谱测井中表现为水下分流河道间页岩中的铀和钍含量均明显低于三角洲平原；③菱铁矿的光电吸收截面指数（Pe）介于14.686～14.510，长英质矿物和黏土矿物的光电吸收截面指数分别介于1.682～2.994和1.56～3.18[21]，水下分流河道间页岩中菱铁矿的大量发育使得地层的光电吸收截面指数明显升高，一般介于3.8～5.0（图3b）。

2.4　三角洲平原

研究区三角洲平原亚相由分流河道微相和分流间湾微相组成，页岩主要发育在分流间湾微相中。

分流间湾页岩的颜色类型多样，包括深灰色、灰色和杂色（图2d），指示着其在沉积期的水体波动性较强，覆水环境和暴露环境均有发育。受分流河道洪泛作用的影响，页岩中长英质的含量相对较高。分流间湾页岩中菱铁矿结核少见且分布较为局限。

分流间湾页岩的岩石物理特征与水下分流河道间页岩明显不同，表现为：①分流间湾页岩中易导电矿物菱铁矿的发育程度远小于水下分流河道间页岩，造成其的测井电阻率明显高于水下分流河道间页岩；②菱铁矿的欠发育使得地层中放射性元素含量受稀释的程度减弱，在自然伽马能谱测井中表现为分流间湾页岩的铀和钍含量明显较水下分流河道间页岩高；③菱铁矿的欠发育也降低了地层的光电吸收截面指数值，造成其总体上明显低于水下分流河道间页岩，一般介于3.0～4.0，仅在局部菱铁矿集中发育的层位出现异常高值（图3b）。

3　沉积演化

晚石炭世格舍尔期，华北板块的海侵活动达到最高峰[22]，太原组下段发育在于该背景下，页岩主要形成于潟湖环境，测井上表现出高自然伽马和高电阻率的特点。早二叠世早期，晚古生代冰川活动的强度达到高峰，大陆

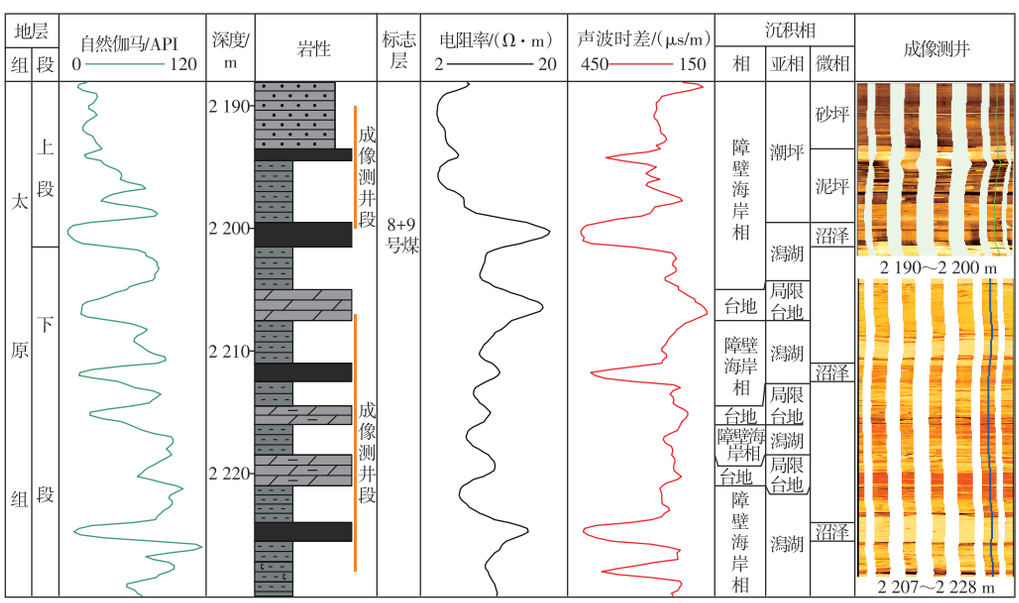

a. 障壁海岸相

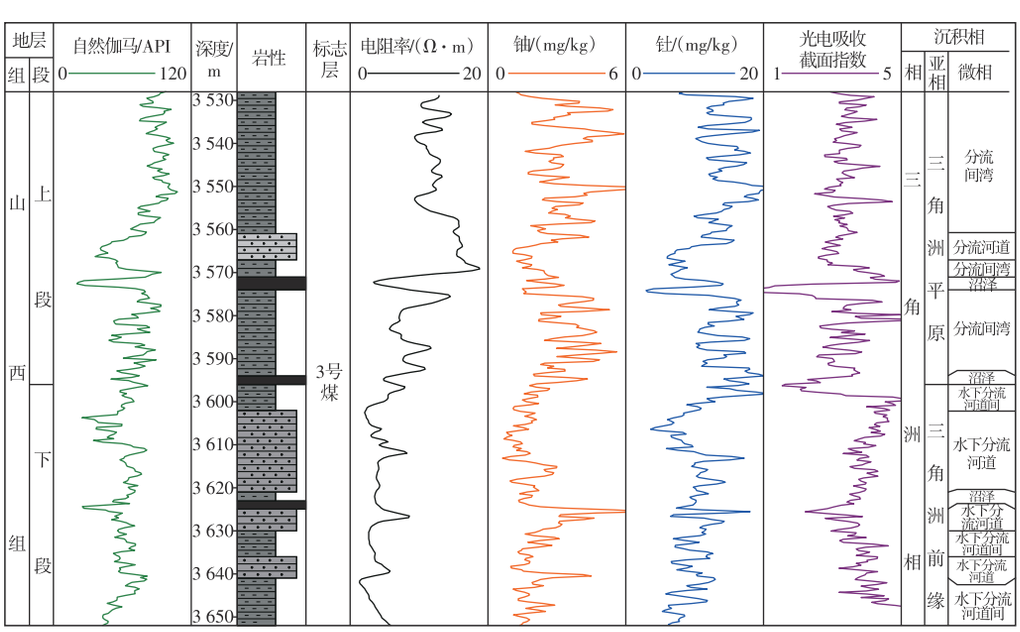

b. 三角洲相

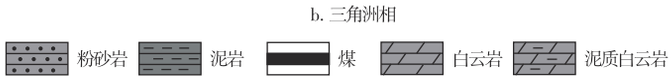

图3　不同沉积环境页岩测井响应

Fig. 3　Logging responses of shales from different sedimentary environments

冰盖广泛分布于冈瓦纳大陆的高纬度以及中纬度高原或高地地区[23]，冰川的发育导致全球海平面大幅下降，太原组上段发育在该背景下，表现页岩沉积环境突然由太原组下段的潟湖转变为上段的潮坪，测井上表现为由高自然伽马高电阻率转变为低自然伽马和低电阻率。随着早二叠世华北北部物源区隆升作用不断加剧，陆源碎屑供给能力增强，研究区的沉积环境由障壁海岸相转变为三角洲相，山西组下段主要发育三角洲前缘亚相，页岩形成于水下分流河道间环境，测井上具有低电阻率的特点随着三角洲由北向南的不断推进，山西组上段主要发育三角洲平原亚相，页岩主要形成于分流间湾环境，测井上表现为电阻率值较水下分流河道间页岩明显增大。

总体而言，研究区太原组—山西组经历了晚古生代海侵作用由高峰向衰退的转化过程；在此背景下发育的页岩的沉积环境经历了由障壁海岸向三角洲转变的过程，页岩自下而上分别发育在潟湖、潮坪、三角洲前缘和三角洲平原亚相中。

4　沉积有机质特征

4.1　有机质丰度

有机质丰度是衡量烃源岩生烃能力的物质基础[24]，通过对有机质丰度进行评价，可以明确烃源岩生烃母质的数量，为资源量计算和资源评价提供依据。

在对研究区上古生界煤系页岩进行精细沉积环境分析的基础上，对不同环境下发育的页岩的有机质丰度进行对比研究。通过对46块潟湖页岩样品进行总有机碳分析可知，其总有机碳含量分布范围较大，介于0.11%～19.30%，平均为3.81%（图4a）；通过对53块潮坪页岩样品进行总有机碳分析可知，其总有机碳含量分布范围同样较大，介于0.70%～17.99%，平均为4.18%（图4b）；通过对29块水下分流河道间页岩进行总有机碳分析可知，其总有机碳含量分布范围适中，介于0.29%～5.91%，平均为2.45%（图4c）；通过对62块分流间湾页岩进行总有机碳分析可知，其总有机碳含量分布适中，介于0.03%～7.36%，平均为2.21%（图4d）。通过对比不同环境下页岩总有机碳的丰度特征，可知潮坪页岩总有机碳的平均丰度最高，潟湖页岩次之，之后为水下分流河道间页岩，分流间湾页岩的总有机碳平均丰度最低。总体而言，障壁海岸相中页岩的有机质丰度要高于三角洲相。

4.2　有机质类型

有机质类型是对有机显微组分组成的综合评价，为影响油气生成的关键因素和评价烃源岩的重要指标。研究采用岩石热解参数氢指数和最大热解峰温度的关系识别有机质类型。潟湖页岩、潮坪页岩、水下分流河道间页岩和分流间湾页岩有机质类型组成相似，主要为Ⅲ型，同时包含部分$Ⅱ_2$型（图4e），指示着有机质来源包含陆源高等植物和低等水生生物双重输入，并以陆源高等植物为优势输入。同时，页岩中的有机质显微组分特征也指示着双重输入的特点，煤系页岩中的有机质显微组分通常以镜质组和惰质组为主，指示着陆生高等植物的输入；荧光条件下可见薄片中发育有不定形条带状的腐泥组组分，具有明显的亮黄色荧光显示（图5），指示着有机质母质包括低等水生生物。

4.3　有机质成熟度

有机质的成熟度是用来判断烃源岩是否有效的参数，为评价页岩生烃量和资源前景的重要依据[24]。研究

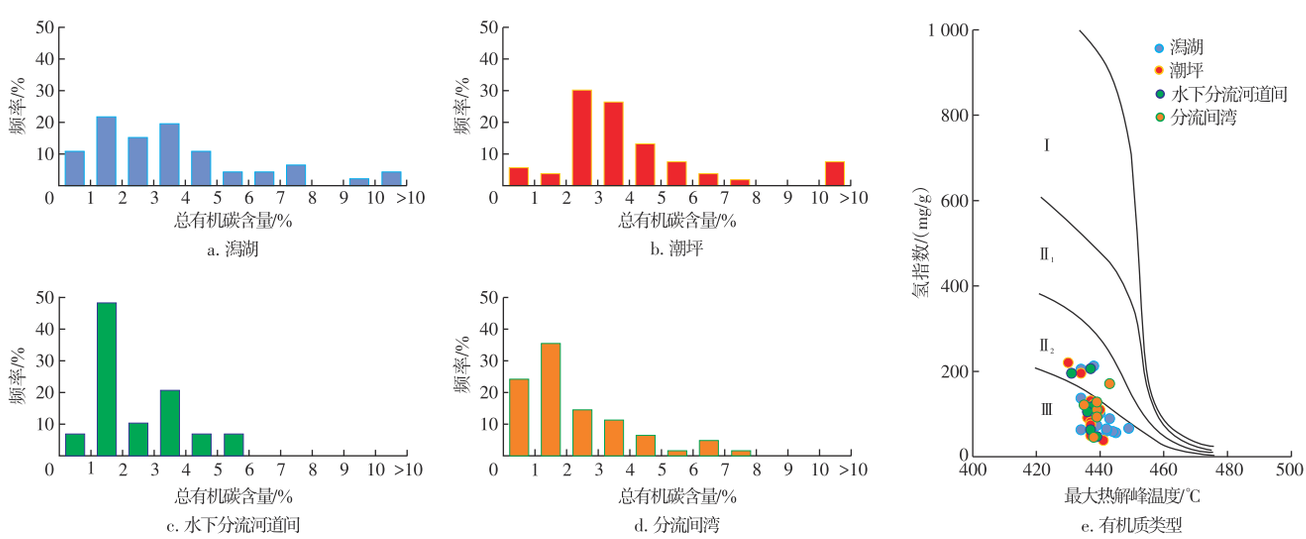

图4　黄骅坳陷煤系地层页岩有机质丰度与类型

Fig. 4　Organic matter abundance and types of coal-measure shales in Huanghua Depression

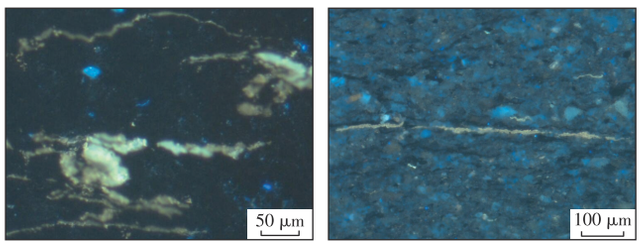

a. 页岩中的腐泥组，太原组上段，G16井，2 198.50 m，荧光　　b. 页岩中的腐泥组，太原组下段，G16井，2 209.98 m，荧光

图5　黄骅坳陷煤系地层页岩有机质显微组分

Fig. 5　Maceral composition of organic matter in coal-measure shales of Huanghua Depression

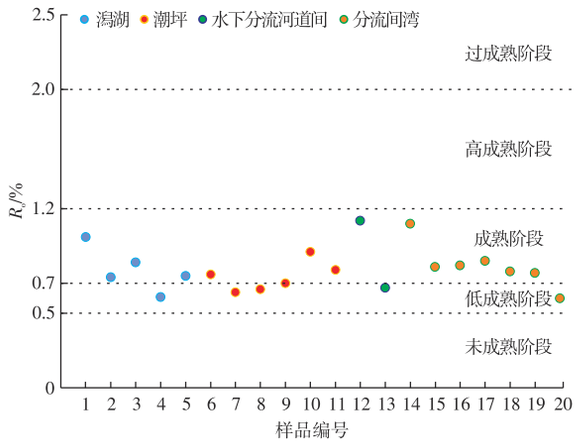

注：R_o为镜质体反射率，%。

图6　黄骅坳陷煤系地层页岩镜质体反射率

Fig. 6　Vitrinite reflectance of coal-measure shales in Huanghua Depression

通过镜质体反射率(R_o)表征有机质的成熟度。

研究区上古生界煤系页岩R_o介于0.60%～1.12%，平均为0.79%。根据R_o<0.5%、0.5%～<0.7%、0.7%～<1.2%、1.2%～2.0%、>2.0%可以将有机质的成熟度划分为未成熟、低成熟、成熟、高成熟及过成熟5个演化阶段，将研究区上古生界煤系页岩样品的R_o数据投入到成熟度判别图版中，可知其处于低成熟—成熟的演化阶段(图6)。

5　沉积控制的页岩富气潜力

5.1　页岩富气层段

综合以上分析，认为黄骅坳陷中潮坪页岩的页岩气富气潜力最大。首先，潮坪页岩的总有机碳含量平均为4.18%，略高于潟湖页岩，但明显高于水下分流河道间页岩和分流间湾页岩，有利于页岩气的生成。潮坪页岩中长英质颗粒较为丰富，包括长英质条带和零散分布的长英质颗粒，导致页岩大孔和微细孔隙均较为发育，有利于页岩气的储集；同时，潮坪页岩中长英质颗粒的发育增加了岩石中脆性矿物的含量，增强了其可改造性，有利于后期页岩气开发过程中的压裂改造。通过沉积相的垂向演化分析可知，黄骅坳陷潮坪沉积主要发育在太原组上段，而页岩主要发育在潮坪沉积中的泥坪微相。通过气测显示也能指示页岩气的富气层段，总体来看，太原组的气测显示明显好于山西组(图7)，这与两层段的富有机质特征的差异性相符。对于太原组来说，上段的气测显示总体好于下段(图7a)，

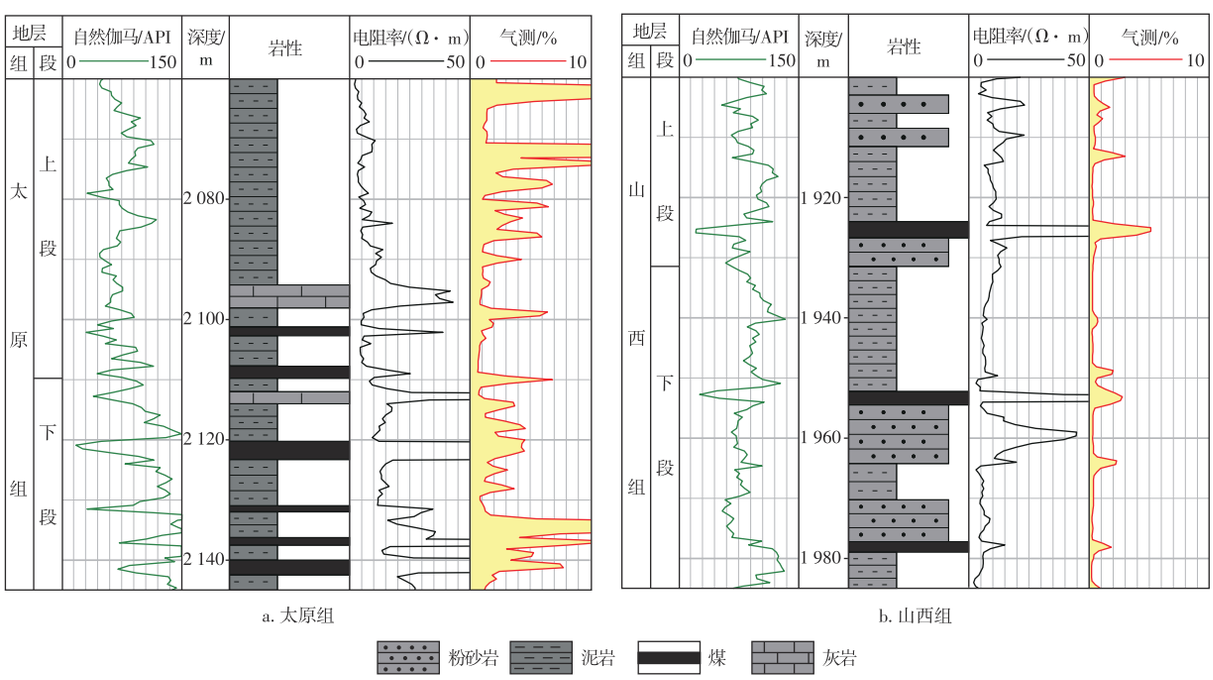

a. 太原组　　b. 山西组

图7　黄骅坳陷GG1井气测显示

Fig. 7　Gas logging of well GG1 in Huanghua Depression

指示着太原组上段的潮坪成因页岩是最具潜力的页岩富气层段。

5.2　页岩气有利区

早二叠世太原组上段沉积期，华北的海侵作用主要来自盆地的东南方向，黄骅坳陷的大部分地区均发育潮坪沉积，仅在东部的埕海地区发育障壁岛和潟湖沉积，而泥坪主要发育在黄骅坳陷的西部，呈北东—南西向展布（图8），在其范围内的沧县隆起、东光潜山、乌马营潜山、孔店潜山、北大港潜山、歧北潜山和歧南潜山是页岩气勘探的有利区域。

6　结论

1）黄骅坳陷太原组—山西组页岩形成于障壁海岸环境和三角洲环境，其中障壁海岸相中发育潟湖页岩和潮坪页岩，三角洲相中发育水下分流河道间页岩和分流间湾页岩。

2）黄骅坳陷潟湖页岩主要发育在太原组下段，潮坪页岩主要发育在太原组上段，水下分流河道间页岩主要发育在山西组下段，分流间湾页岩主要发育在山西组上段；黄骅坳陷太原组—山西组页岩自下而上总体经历了由障壁海岸相到三角洲相的转变，响应着晚古生代海侵

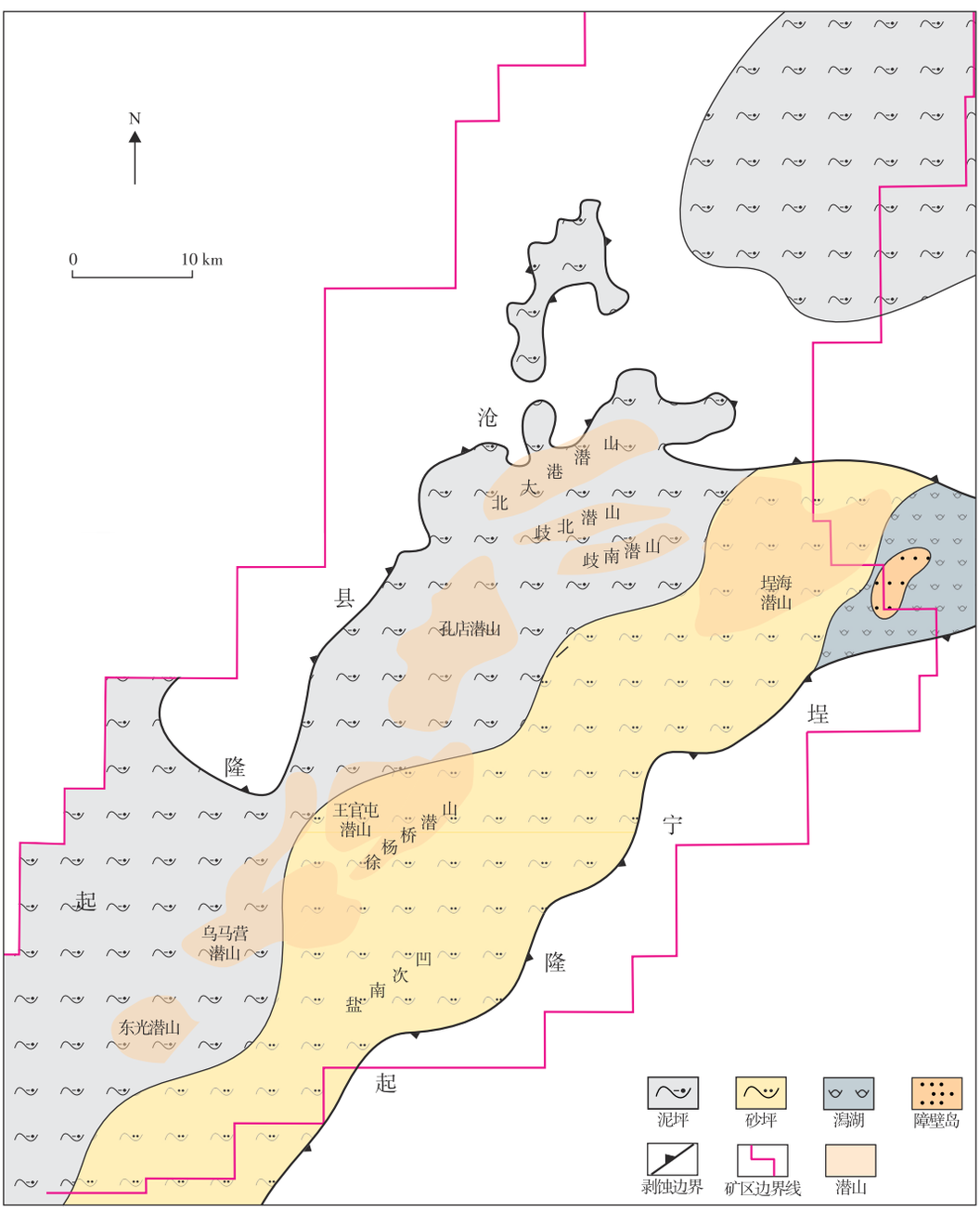

图8　黄骅坳陷太原组上段沉积相

Fig. 8　Sedimentary facies of upper member of Taiyuan Formation in Huanghua Depression

作用由高峰到衰退的过程。

3）黄骅坳陷太原组—山西组页岩以障壁海岸相页岩有机质丰度最高,其次为三角洲相页岩。不同沉积环境中发育的页岩有机质类型类似,主要为Ⅲ型,同时包含部分$Ⅱ_2$型,有机质总体处于低成熟—成熟的演化阶段。潮坪页岩是页岩气勘探的有利层段。

4）太原组上段的潮坪页岩是页岩气勘探的有利层段,位于黄骅坳陷西部的沧县隆起、东光潜山、乌马营潜山、孔店潜山、北大港潜山、歧北潜山和歧南潜山是页岩气勘探的有利地带。

参考文献

[1] SCHIEBER J, SOUTHARD J B. Bedload transport of mud by floccule ripples: Direct observation of ripple migration processes and their implications[J]. Geology, 2009, 37(6): 483-486.

[2] 梁超, 吴靖, 姜在兴, 等. 有机质在页岩沉积成岩过程及储层形成中的作用[J]. 中国石油大学学报(自然科学版), 2017, 41(6): 1-8.
LIANG Chao, WU Jing, JIANG Zaixing, et al. Significances of organic matters on shale deposition, diagenesis process and reservoir formation[J]. Journal of China University of Petroleum (Edition of Natural Science), 2017, 41(6): 1-8.

[3] 宋明水, 刘惠民, 王勇, 等. 济阳坳陷古近系页岩油富集规律认识与勘探实践[J]. 石油勘探与开发, 2020, 47(2): 225-235.
SONG Mingshui, LIU Huimin, WANG Yong, et al. Enrichment rules and exploration practices of Paleogene shale oil in Jiyang Depression, Bohai Bay Basin, China[J]. Petroleum Exploration and Development, 2020, 47(2): 225-235.

[4] 胡钦红, 张宇翔, 孟祥豪, 等. 渤海湾盆地东营凹陷古近系沙河街组页岩油储集层微米—纳米级孔隙体系表征[J]. 石油勘探与开发, 2017, 44(5): 681-690.
HU Qinhong, ZHANG Yuxiang, MENG Xianghao, et al. Characterization of micro-nano pore networks in shale oil reservoirs of Paleogene Shahejie Formation in Dongying Sag of Bohai Bay Basin, East China[J]. Petroleum Exploration and Development, 2017, 44(5): 681-690.

[5] 聂海宽, 张培先, 边瑞康, 等. 中国陆相页岩油富集特征[J]. 地学前缘, 2016, 23(2): 55-62.
NIE Haikuan, ZHANG Peixian, BIAN Ruikang, et al. Oil accumulation characteristics of China continental shale[J]. Earth Science Frontiers, 2016, 23(2): 55-62.

[6] 侯中帅, 陈世悦, 桑树勋, 等. 渤海湾盆地上古生界泥岩地球化学特征[J]. 煤炭学报, 2020, 45(4): 1457-1472.
HOU Zhongshuai, CHEN Shiyue, SANG Shuxun, et al. Geochemical characteristics of upper Paleozoic mudstone in Bohai Bay basin[J]. Journal of China Coal Society, 2020, 45(4): 1457-1472.

[7] 付金华, 李士祥, 徐黎明, 等. 鄂尔多斯盆地三叠系延长组长7段古沉积环境恢复及意义[J]. 石油勘探与开发, 2018, 45(6): 936-946.
FU Jinhua, LI Shixiang, XU Liming, et al. Paleo-sedimentary environmental restoration and its significance of Chang 7 Member of Triassic Yanchang Formation in Ordos Basin, NW China[J]. Petroleum Exploration and Development, 2018, 45(6): 936-946.

[8] 陈世悦, 张顺, 王永诗, 等. 渤海湾盆地东营凹陷古近系细粒沉积岩岩相类型及储集层特征[J]. 石油勘探与开发, 2016, 43(2): 198-208.
CHEN Shiyue, ZHANG Shun, WANG Yongshi, et al. Lithofacies types and reservoirs of Paleogene fine-grained sedimentary rocks in Dongying Sag, Bohai Bay Basin[J]. Petroleum Exploration and Development, 2016, 43(2): 198-208.

[9] 赵建华, 金之钧, 金振奎, 等. 四川盆地五峰组—龙马溪组页岩岩相类型与沉积环境[J]. 石油学报, 2016, 37(5): 572-586.
ZHAO Jianhua, JIN Zhijun, JIN Zhenkui, et al. Lithofacies types and sedimentary environment of shale in Wufeng-Longmaxi Formation, Sichuan Basin[J]. Acta Petrolei Sinica, 2016, 37(5): 572-586.

[10] 侯中帅, 陈世悦, 郭宇鑫, 等. 华北中南部博山地区上古生界沉积相与沉积演化特征[J]. 沉积学报, 2018, 36(4): 731-742.
HOU Zhongshuai, CHEN Shiyue, GUO Yuxin, et al. Sedimentary facies and their evolution characteristics of upper Paleozoic in Zibo Boshan area, central and southern region of North China[J]. Acta Sedimentologica Sinica, 2018, 36(4): 731-742.

[11] 赵仁文, 肖佃师, 卢双舫, 等. 高—过成熟陆相断陷盆地页岩与海相页岩储层特征对比: 以徐家围子断陷沙河子组和四川盆地龙马溪组为例[J]. 油气藏评价与开发, 2023, 13(1): 52-63.
ZHAO Renwen, XIAO Dianshi, LU Shuangfang, et al. Comparison of reservoir characteristics between continental shale from faulted basin and marine shale under high-over mature stage: Taking Shahezi Formation in Xujiaweizi faulted basin and Longmaxi Formation in Sichuan Basin as an example[J]. Petroleum Reservoir Evaluation and Development, 2023, 13(1): 52-63.

[12] 林中凯, 张少龙, 李传华, 等. 湖相页岩油地层岩相组合类型划分及其油气勘探意义: 以博兴洼陷沙河街组为例[J]. 油气藏评价与开发, 2023, 13(1): 39-51.
LIN Zhongkai, ZHANG Shaolong, LI Chuanhua, et al. Types of shale lithofacies assemblage and its significance for shale oil exploration: A case study of Shahejie Formation in Boxing Sag[J]. Petroleum Reservoir Evaluation and Development, 2023, 13(1): 39-51.

[13] 李继东, 许书堂, 杨玉娥, 等. 东濮凹陷胡古2气藏成藏条件分析[J]. 断块油气田, 2015, 22(4): 450-453.
LI Jidong, XU Shutang, YANG Yu'e, et al. Forming condition analysis of Hugu 2 gas reservoir in Dongpu Depression[J]. Fault-Block Oil & Gas Field, 2015, 22(4): 450-453.

[14] 赵贤正, 蒲秀刚, 姜文亚, 等. 黄骅坳陷古生界含油气系统勘探突破及其意义[J]. 石油勘探与开发, 2019, 46(4): 621-632.
ZHAO Xianzheng, PU Xiugang, JIANG Wenya, et al. An exploration breakthrough in Paleozoic petroleum system of Huanghua Depression in Dagang Oilfield and its significance[J]. Petroleum Exploration and Development, 2019, 46(4): 621-632.

[15] 匡立春, 董大忠, 何文渊, 等. 鄂尔多斯盆地东缘海陆过渡相页岩气地质特征及勘探开发前景[J]. 石油勘探与开发, 2020, 47(3): 435-446.
KUANG Lichun, DONG Dazhong, HE Wenyuan, et al. Geological characteristics and development potential of transitional shale gas in the east margin of the Ordos Basin, NW China[J]. Petroleum Exploration and Development, 2020, 47(3): 435-446.

[16] 陈世悦, 马帅, 贾贝贝, 等. 渤海湾盆地石炭—二叠系含煤岩系沉积环境及其展布规律[J]. 煤炭学报, 2018, 43(增刊2): 513-523.
CHEN Shiyue, MA Shuai, JIA Beibei, et al. Sedimentary

environment and distribution law of Carboniferous-Permian coal-bearing series in Bohai Bay Basin[J]. Journal of China Coal Society, 2018, 43(Suppl. 2): 513-523.

[17] 汪珊, 张宏达, 孙继朝, 等. 渤海湾黄骅裂谷盆地深层水形成演化[M]. 北京: 地质出版社, 2005.
WANG Shan, ZHANG Hongda, SUN Jichao, et al. Evolution of deep groundwater at Huanghua rift basin in Bohai bay[M]. Beijing: Geological Publishing House, 2005.

[18] 侯中帅, 陈世悦, 鄢继华, 等. 大港探区上古生界沉积特征与控制因素[J]. 地球科学, 2017, 42(11): 2055-2068.
HOU Zhongshuai, CHEN Shiyue, YAN Jihua, et al. Sedimentary characteristics and control factors of upper Palaeozoic in Dagang exploration area[J]. Earth Science, 2017, 42(11): 2055-2068.

[19] 中国石油勘探与生产分公司. 低阻油气藏测井评价技术及应用[M]. 北京: 石油工业出版社, 2009.
Petrochina Exploration and Production Company. Logging evaluation technology and application of low resistance reservoirs[M]. Beijing: Petroleum Industry Press, 2009.

[20] 侯中帅, 梁钊, 陈世悦. 华北东部晚古生代过渡相煤系地层低阻成因、控制因素与地质意义[J]. 煤炭科学技术, 2024, 52(3): 159-168.
HOU Zhongshuai, LIANG Zhao, CHEN Shiyue. Genesis, controlling factors and geological significance of low resistivity in Late Paleozoic transitional coal measures in Eastern North China[J]. Coal Science and Technology, 2024, 52(3): 159-168.

[21] 斯伦贝谢公司. 测井解释常用岩石矿物手册[M]. 北京:石油工业出版社, 1998.
Schlumberger. A handbook of commonly used rocks and minerals for logging interpretation[M]. Beijing: Petroleum Industry Press, 1998.

[22] 吕大炜, 刘海燕, 孟彦如, 等. 华北板块晚古生代海侵事件沉积类型及分布[J]. 中国煤炭, 2014, 40(8): 35-38.
LYU Dawei, LIU Haiyan, MENG Yanru, et al. Sediment types and distribution of transgression events in Late Paleozoic Era in North China plate[J]. China Coal, 2014, 40(8): 35-38.

[23] 杨江海, 颜佳新, 黄燕. 从晚古生代冰室到早中生代温室的气候转变: 兼论东特提斯低纬区的沉积记录与响应[J]. 沉积学报, 2017, 35(5): 981-993.
YANG Jianghai, YAN Jiaxin, HUANG Yan. The earth's penultimate icehouse-to-greenhouse climate transition and related sedimentary records in low-latitude regions of eastern Tethys[J]. Acta Sedimentologica Sinica, 2017, 35(5): 981-993.

[24] 许婷, 许锋, 郭玉华, 等. 陕南西乡—镇巴地区下古生界页岩有机地球化学特征[J]. 东北石油大学学报, 2019, 43(4): 59-68.
XU Ting, XU Feng, GUO Yuhua, et al. Organic geochemical characteristics of the lower Paleozoic shales in Xixiang-Zhenba area, southern Shaanxi[J]. Journal of Northeast Petroleum University, 2019, 43(4): 59-68.

(编辑 李青)